

TRIALS OF BEAM-BASED SEXTUPOLE CALIBRATION THROUGH 2ND ORDER DISPERSION

D. K. Olsson*, Å. Andersson, M. Sjöström, MAX IV Laboratory, Lund University, Lund, Sweden

Abstract

In order to achieve nominal performance in terms of the dynamic aperture and lifetime of a storage ring, it is important to be able to characterise and correct its second order optics. At the MAX IV 3 GeV storage ring in Lund, Sweden, the linearity of the 2nd order dispersion with chromatic sextupole field strengths has been utilised to investigate the sextupole circuits. The beating induced in the 2nd order dispersion when reducing the strength of a sextupole magnet can be compared to the beating in simulations. From this a beam-based sextupole calibration curve can be found. This work was inspired by similar work done at ESRF [1].

THE MAX IV 3 GEV STORAGE RING LATTICE

The MAX IV 3 GeV storage ring lattice consists of 20 identical achromats. Each achromat has five sextupole magnet families (see Fig. 1), each on a separate circuit by family and achromat. The SDend, SFi, SFo, and SFm families consist of two magnets connected in series, while the SD family consists of 10 in series. The SFi circuit in achromat 8 is split up for BPM offset experiments, resulting in a total of 101 separate sextupole circuits [2].

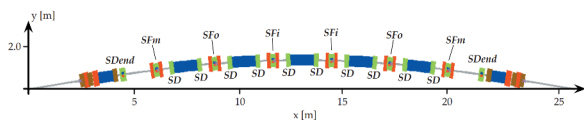


Figure 1: Sextupoles of the MAX IV 3 GeV storage ring achromats. [2]

The linear optics has been corrected using LOCO, and the machine functions can be found in [4]. There, the maximum amplitude of the horizontal beta beat is reported to be $\sim 1.9\%$, and the dispersion beating $\sim 6.2\%$. At the time of measuring, the horizontal beta beat was slightly higher at $\sim 2.8\%$.

Prior to these investigations the non-linear optics of the machine had been optimised using RCDS in order to increase horizontal kick resilience [4], and the chromaticity corrected to $+1/+1$. Due to time constraints the optimisation used global sextupole and octupole family values as optimisation parameters.

THEORY

The second order dispersion function, η_1 , is given by [3]:

$$\eta_1 = \frac{\sqrt{\beta(s)}}{2 \sin \pi \nu} \int_s^{s+L} \sqrt{\beta(\zeta)} f_1(\zeta) \cos [\nu \pi + \varphi(s) - \varphi(\zeta)] d\zeta$$

$$f_1 = -h + (2h^2 - k + h' \eta_0') \eta_0 + (2hk - h^3 + \frac{1}{2}m) \eta_0^2 + \frac{1}{2} h \eta_0'^2 \quad (1)$$

where h , the dipole bending curvature, k , the normalised quadrupole strength, and m , the normalised sextupole strength, are all functions of the longitudinal position, s .

From Eq. (1) we get that the second order dispersion is linear with respect to the sextupole fields of the lattice. Thus, a change in the 2nd order dispersion, induced by a change in sextupole strength, can be used to derive the change of sextupole strength.

METHOD

The 2nd order dispersion of the MAX IV 3 GeV storage ring was simulated in Accelerator Toolbox using full 6-dimensional particle tracking. The procedure used was the same as the one later used to measure on the machine. The accelerating RF was shifted between -500 Hz to 500 Hz in 100 steps of 10 Hz. At each BPM, a polynomial was fitted to the dispersive orbit vs change in momentum. The 2nd order dispersion at each BPM is the quadratic coefficient of this polynomial, while the linear coefficient is the 1st order dispersion.

In order to properly extract the 2nd order component of the dispersive orbit the polynomial to fit needs to be of a high enough order, at a certain shift in RF, so that higher order components do not affect the 2nd order component. The order also needs to be low enough so that there is little risk of over-fitting to the BPM noise present in the real measurement.

For a shift of ± 500 Hz in accelerating RF, fitting a third order polynomial is sufficient to bring the residuals down to a level set by the BPM noise at cold beam, $\sigma = 0.4 \mu\text{m}$ (see Fig. 2).

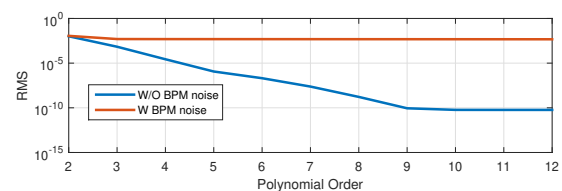


Figure 2: RMS when fitting a polynomial of a certain order to the dispersive orbit in each BPM. The RMS becomes dominated by BPM noise, $\sigma = 0.4 \mu\text{m}$, at 3rd order.

* david_k.olsson@maxiv.lu.se

Content from this work may be used under the terms of the CC BY 3.0 licence (© 2019). Any distribution of this work must maintain attribution to the author(s), title of the work, publisher, and DOI

The change in accelerating frequency was converted to a change in momentum using a momentum dependent MCF, $\alpha(\delta)$, from simulation. The momentum dependence of α was small, but included nonetheless. The BPM readings of the dispersive orbit was corrected for BPM non-linearities using a polynomial map calculated from a boundary element method [5]. A fourth order polynomial was fitted to the orbit excursion in each BPM as a function of momentum deviation.

When modulating the strength of a single sextupole circuit, a 2nd order dispersion beating pattern appears. For each of the measured 2nd order dispersion beating patterns the strength of the corresponding magnet can be tuned in the model until the beating pattern of the model 2nd order dispersion matches the measured. From this, we get a relative magnet calibration where a certain change in current corresponds to a certain change in sextupole field strength.

As given by Eq. (1), the 2nd order dispersion depends quadratically on the 1st order dispersion, and linearly on the beta functions, at the location of the magnet. Thus, the signal-to-noise is higher at a location of high 1st order dispersion and beta function.

MEASUREMENTS

A typical example of the measured data at a low dispersion BPM and a high dispersion BPM can be seen in Fig. 3 and Fig. 4 respectively.

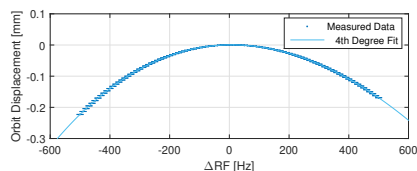


Figure 3: Dispersive orbit in a low 1st order dispersion BPM. The errorbars are given by the STD of 10 BPM readings.

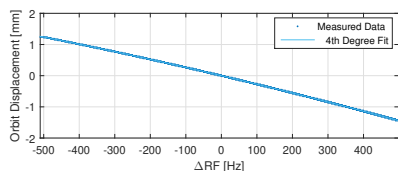


Figure 4: Dispersive orbit in a high 1st order dispersion BPM. The errorbars are given by the STD of 10 BPM readings.

The measured 2nd order dispersion of the MAX IV 3 GeV ring can be seen in Fig. 5. When reducing the strength of a single SFi magnet a clear beating pattern appears (see Fig. 6). A subset of magnets belonging to the SDend and SFi family were investigated, and are presented here.

Resulting Calibration Curve

The fit at a location of high dispersion can be seen in Fig. 7, and at low dispersion in Fig. 8.

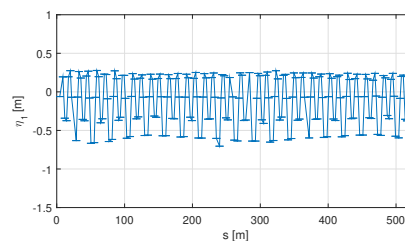


Figure 5: Initial measured 2nd order dispersion of the MAX IV 3 GeV. The errorbars are given by the STD of 10 measurements.

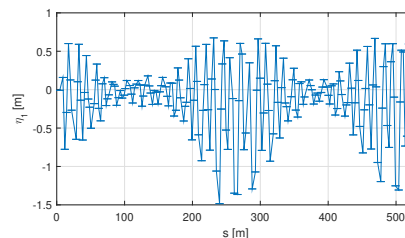


Figure 6: Measured 2nd order dispersion of the MAX IV 3 GeV after reducing a single SFi magnet to zero. The errorbars are given by the STD of 10 measurements.

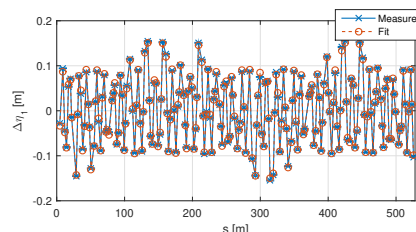


Figure 7: Measured and simulated 2nd order dispersion beat induced by a SFi magnet, which is at a location of high dispersion. The errorbars are given by the STD of 10 measurements.

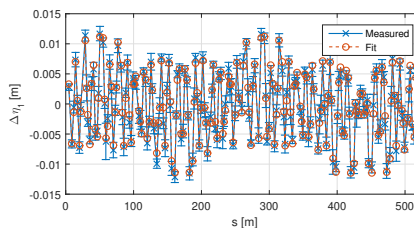


Figure 8: Measured and simulated 2nd order dispersion beat induced by a SDend circuit, which is at a location of low dispersion. The errorbars are given by the STD of 10 measurements.

From the fitted 2nd order dispersion a calibration curve could be calculated for each of the two examples above. In the case of the high dispersion sextupole (see Fig. 9), calibration curves calculated from 2nd order dispersion are not greatly affected by noise. The sextupole also appears to be $\sim 11.5\%$ stronger compared to the rotating coil calibration

curve. In the case of the lower dispersion sextupole (see Fig. 10), the dispersion calibration appears to match the rotating coil measurement fairly well. However, measurements on this sextupole appear to be more affected by noise.

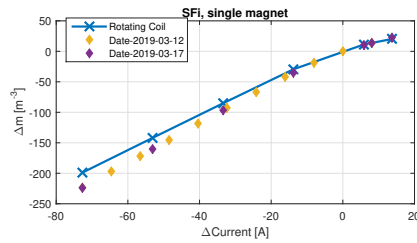


Figure 9: Calibration from rotating coil measurements as well as from 2nd order dispersion measurements. The sextupole used is a single sextupole, SFi, at a location of high dispersion.

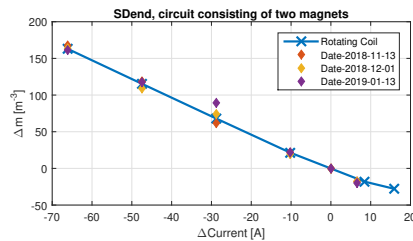


Figure 10: Calibration from rotating coil measurements as well as from 2nd order dispersion measurements. The sextupoles used are a circuit of two magnets, SDend, at a location of low dispersion.

Chromaticity Measurements

The 2nd order dispersion calibration curve in Fig. 9 deviates significantly from the rotating coil measurement. In order to ascertain whether this measurement is accurate, the chromaticity of the machine was measured at the same magnet currents as the 2nd order dispersion measurements. The measured chromaticities, along with the expected chromaticities assuming the sextupole follows either the rotating coil or 2nd order dispersion calibration curve, can be seen in Fig. 11.

Sources of Error

From the chromaticity measurement it appears that the rotating coil measurement can better predict the change in chromaticity when decreasing the sextupole current. This might be explained by errors in the linear optics. The 2nd order dispersion's dependence on beta function is linear, while its dependence on 1st order dispersion is quadratic. Assuming an equal distribution of errors in both the beta and dispersion functions at the location of the sextupole, a beating of $\sim 2.7\%$ from nominal is sufficient to explain the disparity between the rotating coil and 2nd order dispersion calibrations. This value is in the range of the beta and dispersion beating of the MAX IV 3 GeV storage ring at the time

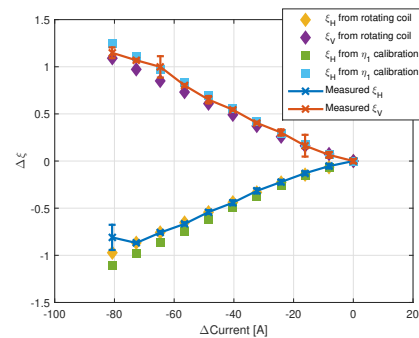


Figure 11: Measured chromaticity when decreasing the strength of the SFi sextupole corresponding to Fig. 9, and the predicted change in chromaticity based on the rotating coil and 2nd order dispersion measurements.

of writing. Since the beating in beta and dispersion function is approximately symmetric around their respective nominal values it will have little effect on the chromaticity.

CONCLUSIONS

The potential of using the 2nd order dispersion of a storage ring to perform a beam based sextupole calibration was explored at the MAX IV 3 GeV storage ring. The reproducibility of the calibration was dependent on the linear optics at the location of the sextupole. At certain sextupoles, the calibration did not match the calibration curves from the rotating coil measurements. Since the 2nd order dispersion calibration curve was not confirmed by chromaticity measurements the discrepancy might be the result of first order optics errors. The errors required to produce this discrepancy are within the ranges of linear optics errors of the MAX IV 3 GeV storage ring at the time of measurements.

Further investigation and measurements are planned in order to ascertain the source of the discrepancy, and whether the 2nd order dispersion sextupole calibration can be used as a complement to the rotating coil measurements.

REFERENCES

- [1] N. Carmignani, "Sextupole Calibrations via Measurements of Off-Energy Orbit Response Matrix and High Order Dispersion", presented at the 25th European Synchrotron Light Source Workshop (ESLS'17), Dortmund, Germany, Nov. 2017.
- [2] "Detailed Design Report", MAX IV Laboratory, Lund, Sweden, Aug. 2010.
- [3] J.-P. Delahaye and J. Jäger, "Variation of the Dispersion Function, Momentum Compaction Factor, and Damping Partition Numbers with Particle Energy Deviation", *Particle Accelerators*, vol. 18, pp. 183-201, 1986.
- [4] P.F. Tavares et al., "Commissioning and first-year operational results of the MAX IV 3 GeV ring", *Journal of Synchrotron Radiation*, vol. 25, pp. 1291-1316, September 2018.
- [5] A. Stella, "Analysis of the DAΦNE Beam Position Monitor with a Boundary Element Method", *DaΦne Technical Note CD-10*, December 1997.